2-1-2016

Trapping Platinum on Ceria: Role of Surface Facets

John Jones

John Jones
Candidate

Nanoscience and Microsystems Engineering
Department

This thesis is approved, and it is acceptable in quality and form for publication:

Approved by the Thesis Committee:

Abhaya Datye, Chairperson

Sivakumar Challa

Fernando Garzon

Trapping Platinum on Ceria: Role of Surface Facets

BY

JOHN JONES

BACHELORS CHEMICAL ENGINEERING

THESIS

Submitted in Partial Fulfillment of the
Requirements for the Degree of

Master of Science

Nanoscience and Microsystems Engineering

The University of New Mexico
Albuquerque, New Mexico

December, 2015

Trapping Platinum on Ceria: Role of Surface Facets

By

John Jones

B.S., Chemical Engineering, University of New Mexico, 2012

M.S. Nanoscience and Microsystems Engineering, University of New Mexico, 2015

ABSTRACT

Supported platinum catalysts are used in the automotive industry for the oxidation of CO, hydrocarbons, and NO_x. Dispersed Pt provides active sites for these reactions to occur. During the use of these catalyst, high temperatures will cause Pt to become volatile and sinter, forming large particles which will lead to a loss of catalytic activity. The study of Pt sintering has been of high priority for the automotive industry along with mechanisms that will reduce the effect of sintering. Developing an understanding of how supports can hinder sintering of Pt will lead to the preparation of more robust catalysts.

A promising support for Pt is CeO_2. Altering the synthesis of CeO_2 can allow for different nanoshapes to be formed which lead to different surface facets being exposed. The three types of nanoshaped CeO_2 synthesized for the catalyst are polyhedra, rods, and cubes, which expose different surface facets. The polyhedra produced expose primarily the (111) and (100) facet while rods expose (111) and cubes expose the (100). These three CeO2 nanoshapes will be tested to discover if one surface facet is able to trap Pt in a dispersed form after aging at high temperature.

Powder catalysts containing CeO_2 were produced to simulate diesel oxidation catalysts. A first set of catalysts was prepared using an incipient wetness technique of La-Al_2O_3 with chloroplatinic acid producing Pt/La-Al_2O_3. This product was then mixed with each of the CeO_2 nanoshapes and aged at 800 ˚C. The resulting products were analyzed to determine if the volatile Pt had sintered or had transferred from the La-Al_2O_3 support and become trapped on the CeO_2 support.

A second set of catalysts was prepared using an incipient wetness technique of each of the CeO_2 nanoshapes with chloroplatinic acid, producing Pt/CeO_2. These catalysts were then aged at 800 ˚C and analyzed to determine the effectiveness of the different exposed surface facets at keeping Pt in a dispersed phase.

Dispersion of Pt after aging at high temperature was shown to have been greatly affected by the type of CeO_2 support used. In both parts of this research, it was found that the CeO_2 cubes, exposing primarily the (100) facet, were not able to keep Pt highly dispersed, allowing for the growth of large Pt particles. The catalysts containing either the CeO2 polyhedra or rods, which exposed the (111) facet, were shown to trap Pt in an atomically dispersed state. This allowed for high catalytic reactivity to be maintained even after aging at high temperature.

Table of Contents

LIST OF FIGURES

CHAPTER 1 - INTRODUCTION

1.1 BACKGROUND

1.1.1 CATALYSIS

The use of catalysts is paramount to many industries to provide an alternative reaction pathway to form a product. Catalysts are able to change the rate of a reaction while emerging from the process unchanged. Roughly one third off the material gross national product of the U.S. involves a catalytic process.[24]They are used in the production of chemicals, oil refining, and pollution control among others.[23]

Heterogeneous catalytic process involves multiple phases. Usually a solid catalyst is used while the reactants and products will be in a liquid or gaseous form. In metallic catalysts, the activity of the catalyst is related to the degree of dispersion of metal particles/atoms. Dispersion is given as

$$D = \frac{N_S}{N_T}$$

where N_S is the number of surface atoms and N_T is the total number of atoms. These exposed surfaced atoms are most often the active face of the catalyst. Having porous structures can lead to high surface areas although if pressure drop is an issue, a catalyst consisting of minute particles dispersed on a support could be used.[24]A common supported catalyst is used by the automotive industry called a catalytic convertor.

The Clean Air Act of 1963 and the Motor Vehicle Air Pollution Control Act in 1965 was the beginning of controlling emissions from motor vehicles. Regulatory

standards on common air pollutants like carbon monoxide and nitrogen oxides would need to be met by manufacturers in order to sell vehicles in the US. Catalytic converters were implemented to help control emissions by converting pollutants to carbon dioxide, water, or nitrogen.

1.1.2 SINTERING

Diesel Oxidation Catalyst (DOC) are used in the automotive industry to help reduce harmful emissions from diesel automotive engines. Pt is a key component utilized in DOC's to oxidize carbon monoxide and hydrocarbons. Pt is dispersed on a support oxide to achieve a high surface area and more active sites for reactions to occur .[5] Under oxidizing conditions at temperatures above 800 ˚C, Pt becomes volatile and begins to sinter and form large particles, leading to loss of catalytic activity.[1, 2, 3] The sintering mechanism is Ostwald Ripening where large particles are more energetically favored over smaller particles. Atoms can move along the support or through the vapor phase to form larger particles as shown in Figure 1. [3]

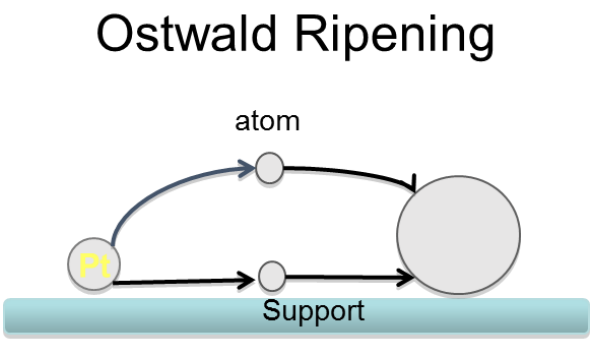

Figure 1: Large particles more energetically favored. Atoms move along support or through vapor phase.

Simonson et al. conducted a study on Pt nanoparticle sintering mechanisms using in situ TEM.[22] Pt nanoparticles were dispersed on a planar amorphous Al_2O_3 support and exposed to air at 650 ˚C. Time-resolved images taken during exposure to high temperature revealed Ostwald ripening as the mechanism for sintering of Pt. The image series clearly shows that the Pt particles are immobile with their size increasing or decreasing. Larger particles will become darker in contrast indicating an increase in particle height while smaller particles will disappear after enough time has elapsed. It should be noted that the size distribution changes during exposure from Gaussian to Liffshitz-Slyozov-Wagner model as large particles are formed at expense of smaller particles. These images can be located in supporting information (S11).

Different support oxides can be used to provide DOCs with characteristics that are beneficial for Pt stabilization. Ceria-based oxides have been used for oxygen storage and have also been shown to help in the stabilization of Pt dispersion.[5] This stabilizing effect is of much interest to vehicle manufactures and has been investigated in several studies, although the Pt-CeO_2 interaction needs to be investigated further. Due to the high cost of Pt, the automotive industry needs to develop a highly sinter resistant catalyst that is able to carry out the desired reactions and lasts the life time of a vehicle.

1.2 PROBLEM STATEMENT

DOCs containing Pt must be able to survive high temperatures in oxidation conditions. If Ostwald Ripening occurs and dispersed Pt sinters into large particles, loss of catalytic activity will occur as the active sites diminish. CeO_2 has been proven to reduce the effect of Ostwald Ripening in several studies, although the different structures

of CeO_2 have not been studied in depth. Studying how Pt sintering is affected by CeO_2 supports displaying different surface facets can benefit the automotive industry in reducing harmful emissions from vehicles while also reducing the amount of Pt necessary.

1.3 RESEARCH QUESTIONS

After considering the problem statement the following research questions were formulated:

- Which surface facet of CeO_2 is most conducive to stabilization of Pt against sintering in air?
- Will CeO_2 help provide high reactivity for CO oxidation for supported Pt?

In answering the proposed research questions, an understanding of CeO_2 surface facets effect on Pt stabilization will be established. This relationship will be explored using characterization techniques like TEM, SEM, and XRD.

The objectives to be accomplished in this study are:

- The synthesis of CeO_2 nanoshapes that exhibit different surface facets
- Synthesis method to develop well dispersed Pt on a powder support of La-Al_2O_3 and CeO_2
- Characterization of catalysts using a variety of techniques
    - TEM, SEM, XRD, BET

- Determine catalytic reactivity to identify the optimal structure of CeO_2 for Pt stabilization

1.4 RESEARCH RATIONAL

Conducting research into long standing technologies is vital to further developing improvements in these fields. By studying the relationships of active sites of a catalyst to the type of support used, a connection can be made to the performance of the catalyst which will lead to improvements in the development of new more robust catalysts. For the Pt-CeO_2 system, determining the surface facet that inhibits Pt sintering most effectively will allow future designs of these catalysts to incorporate these findings. Less Pt will be needed for catalysts and efficiency will be improved, which will reduce costs to manufacturers.

CHAPTER 2 – THEORY AND RESEARCH REVIEW

2.1 CERIUM AND ITS OXIDE CERIA

Cerium is a soft rare earth metal that will oxidize easily. After oxidation cerium will form a stable cerium (IV) oxide (CeO_2). This oxide has a cubic fluorite structure with eight oxygen atoms and four cerium atoms per unit cell shown in Figure 2.

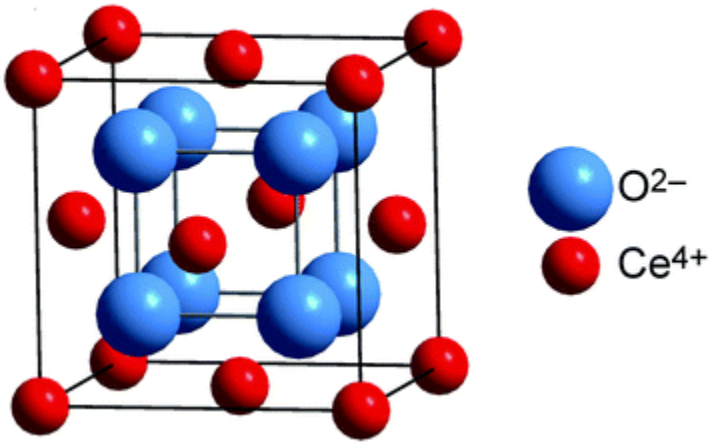

Figure 2: CeO_2 cubic fluorite structure[16]

Partial reduction of CeO_2 leads to the formation of oxygen vacancies. In this reversible reaction, the oxidation state of Ce changes from $Ce^{(IV)}$ to $Ce^{(III)}$. During oxidation, $Ce^{(III)}$ will revert back to $Ce^{(IV)}$. Due to this redox process CeO_2 is able to be used for oxygen storage in catalytic converters.[17]

2.2 PREVIOUS WORK ON CEO_2

CeO_2 is composed of three low index surfaces; (111), (110), and (100). The surface energies increase in the order (111) > (110) > (100).[17] Mai et al. developed a synthesis method to produce CeO_2 cubes, rods, and polyhedra which display primarily (100), (111), and a combination of (100) and (111) respectively.[10] CeO_2 cubes and polyhedra have been imaged extensively and shown to expose certain facets pictured in Figure 3.[18, 19]

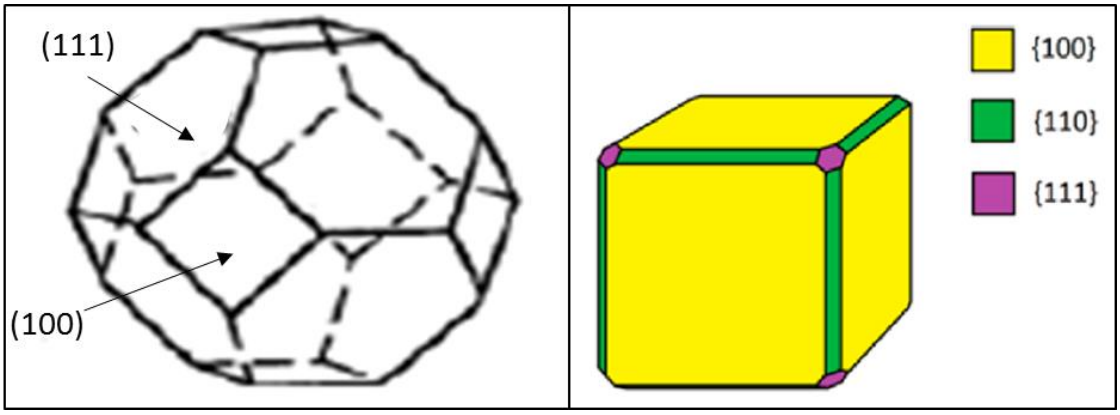

Figure 3: CeO_2 polyhedra on left displaying the (111) and (100) facet. CeO_2 cubes displaying (100) facet on face.

Literature on CeO_2 rods is not as abundant as the cubes or polyhedra. A recent study performed by the Heterogeneous Catalysis Research group at the University of New Mexico indicates the CeO_2 nanorods exhibit primarily the (111) facet. A TEM image of the rods are shown in Figure 4 as having a lattice spacing of 0.317 nm.

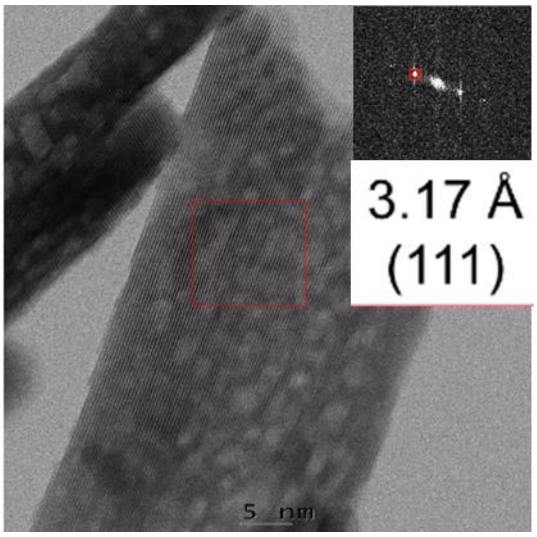

Figure 4: CeO_2 nanorod exposing (111) facet

By utilizing these three nanoshapes, this study will determine which facet is responsible for keeping Pt in a dispersed phase.

2.3 PREVIOUS WORK WITH PLATINUM SINTERING AND TRAPPING

Previous experiments carried out by our research group have indicated a high level of Pt sintering on a La-Al_2O_3 support. A highly dispersed Pt catalyst was formed using an incipient wetness technique which was calcined at 350 ˚C for 5 hours. After aging this catalyst in air at 800 ˚C the Pt particles had formed large particles and CO oxidation reactivity had been greatly diminished. Figure 5 shows data from TEM and XRD which indicate a high level of Pt sintering.

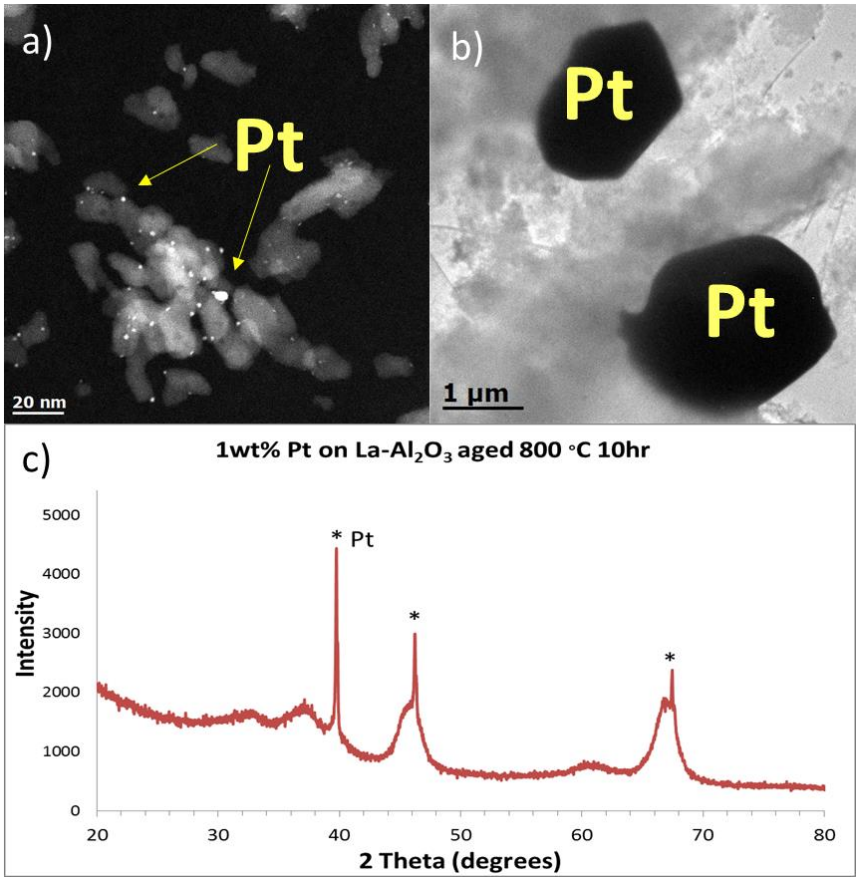

Figure 5. 1 wt.% Pt on La-Al_2O_3 a) TEM after calcination at 350 ˚C for 5 hr., b) TEM after aging at 800 ˚C for 10 hr., c) XRD after aging at 800 ˚C for 10 hr.

Other work involving Pt on Al_2O_3 has shown similar results. Graham et al. made a model NO_x trap with γ-Al2O3 with 2 wt.% Pt and aged in an oxidizing atmosphere

between 600-950 ˚C. The XRD pattern shown in Figure 5 clearly indicates Pt particle growth beginning at 600 ˚C.

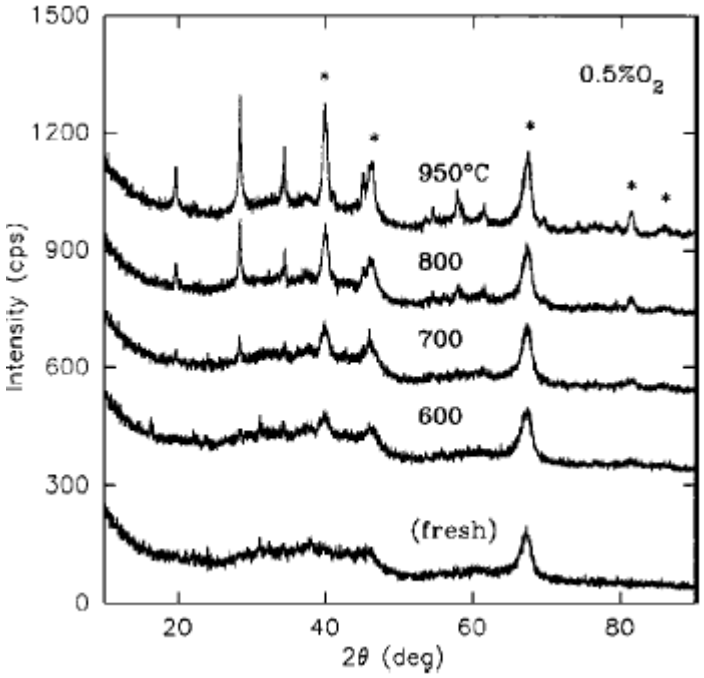

Figure 6: XRD of NOx trap model catalyst after aging in oxidizing atmosphere [2]

Recent work shows that Pt can be trapped by PdO forming Pt-Pd bimetallic particles that slow the rates of sintering. [3, 4] Carrillo et al. deposited PdO on SiO_2 followed by a physical vapor deposition of Pt shown in Figure 7. After an aging treatment at 650 ˚C in air, Pt has formed a bimetallic Pt-Pd nanoparticle. While PdO gets reduced by Pt, we do not expect this to happen with more refractory oxides. Nonetheless, the formation of large particles can be avoided if we could trap the Pt in a dispersed form on a metal oxide.

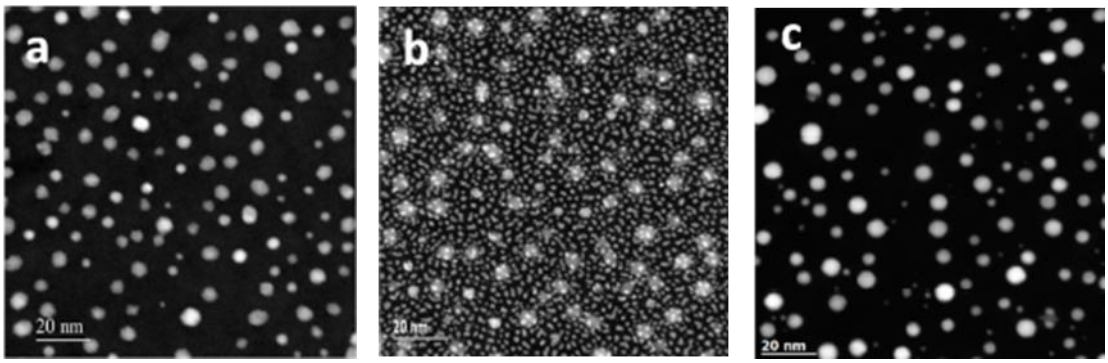

Figure 7: PdO trap for Pt. a) PdO on SiO_2, b) PdO and Pt coexisting, c) Bimetallic Pt-Pd formed.[4]

2.4 PREVIOUS WORK WITH PLATINUM AND CERIA

Ceria is a promising oxide since Nagai et al. have shown that CeO_2 can inhibit sintering of Pt at DOC operating conditions. [5] The typical aging requirements for DOC is at 800 ˚C in air for at least 10 hours. In this study the support used was a mixed oxide of Ce-Zr-Y (CZY) with almost a 50-50 wt.% split between Ce and Zr. Nagai et al. used wet impregnation to create a model powder catalyst with 2 wt.% Pt. TEM images for Pt supported catalysts after aging at 800 ˚C in air show a lack of Pt particles on CZY support while large particles can be found on Al_2O_3 support. Nagai used energy dispersive X-ray to detect Pt on the CZY support indicating the Pt particles remained dispersed after aging. Bera et al. also reached similar conclusions on a combustion synthesized approach of Pt/CeO_2.[15] XRD analysis shows a very small peak for Pt after aging at 800 ˚C for 100 hours while CO oxidation data shows high reactivity unlike Pt/Al_2O_3 samples after aging.

Another study was performed by Wu et al. that indicated the (100) face of the CeO_2 cubes will allow for redispersion of Pt in an alternating oxidation and reduction atmosphere while (111) of CeO_2 octahedral will still sinter, although this was performed

below DOC operating conditions. [6] Bruix et al. performed DFT calculations indicating the square pocket of CeO_2 (100) can stabilize Pt^{2+} by bonding to O^{2-}. [7] Both these studies find the (100) as being responsible for inhibiting the growth of Pt on CeO_2 while Wu et al claimed the (111) surface had little effect on Pt sintering.

A density-functional theory study on Pt/CeO_2 (111) was conducted by Kinch et al. with the (111) surface chosen due to it being the most stable face.[20] It has been shown that the most common defect sites on CeO_2 are oxygen vacancies.[21] Kinch found that although Pt could bind at oxygen vacancies with an energy of 13.55 kcal/mol, the binding energies were much larger in cerium vacancies at 53.22 kcal/mol. It can then be inferred that the facet with the most cerium vacancies should keep Pt from sintering during aging.

CHAPTER 3 – EXPERIMENTAL PROCEDURE

3.1 PT ON LA-AL_2O_3 PREPARATION

A La-Al_2O_3 support was chosen as La has been shown to enhance the thermal stability of γ-Al_2O_3 preventing sintering. [8, 9] The pore volume of La-Al_2O_3 was determined to be 1.0 mL/gram. Using a wet impregnation technique of La-Al_2O_3 with an 8 wt. % solution of chloroplatinic acid (CPA) in water, a 1 wt. % Pt on La-Al_2O_3 was formed. This product was then left to dry in 80˚C air followed by calcination in air at 350˚C for 5 hours. This produced a uniform dispersion of 1 wt. % Pt on La-Al_2O_3 shown in Figure 5a. This sample will be referred to as 'FRESH 1 wt. % Pt on La-Al_2O_3.' Following calcination the sample was loaded in a ceramic boat and placed in a quartz tube. The tube was placed in a furnace and the sample was aged at 800 ˚C for 10 hours in flowing air leading to sintering of Pt and the formation of large crystallites shown in

Figure 5b. XRD data corroborates this as high intensity peaks for Pt are visible in the spectra in Figure 5c. This sample will be referred to as 'AGED 1 wt. % Pt on La-Al_2O_3.'

3.2 SYNTHESIS OF CEO_2 NANOSHAPES

Producing different shapes of CeO_2 utilized two different methods. Both methods used Ce $(NO_3)_3$ $6H_2O$ (99.999%; Sigma-Aldrich) as a precursor. To make CeO_2 polyhedra, Ce $(NO_3)_3$ $6H_2O$ was heated in air at 350 ˚C for 2 hours producing a yellow powder. This powder was then ground using a mortar and pestle to achieve a uniform sample. The polyhedra display primarily the (111) and (100) facets.

Producing CeO_2 rods and cubes required a mixture of Ce $(NO_3)_3$ $6H_2O$, NaOH (EMD), and H_2O to be mixed in a Teflon bottle and sealed tightly in a stainless steel autoclave. To produce CeO_2 rods, the mixture was subjected to a hydrothermal treatment for 24 hours at 100 ˚C and left to cool before opening the autoclave. Producing CeO_2 cubes required a hydrothermal treatment for 24 hours at 180 ˚C and the product was left to cool before opening the autoclave. Both products were then washed with ethanol and water and separated using a centrifuge. The products were then dried in air at 80 ˚C for 12 hours and finally ground with mortar and pestle for uniformity.[10] The CeO_2 rods display the (111) facet while the face of the cubes are the (100) facet.

3.3 CHARACTERIZATION OF CEO_2 NANOSHAPES AND PT/LA-AL_2O_3 CATALYST

Samples were prepared for STEM and HR-TEM by dispersing the CeO_2 nanoshapes in ethanol and mounting on holey carbon grids. Images were taken using a

JEOL 2010F 200kV transmission electron microscope (resolution of 0.14 nm) and a JEOL JEM ARMS200CF 200 kV aberration-corrected (AC) transmission electron microscope (resolution of 0.08 nm). Each nanoshape was then indexed to show which facets are present in each shape pictured in Figure 8. Surface area was determined for each shape of CeO_2 prior to aging using Micromeritics Gemini 2360 surface area analyzer by the multi-point BET method using N_2 adsorption at -196 ˚C.

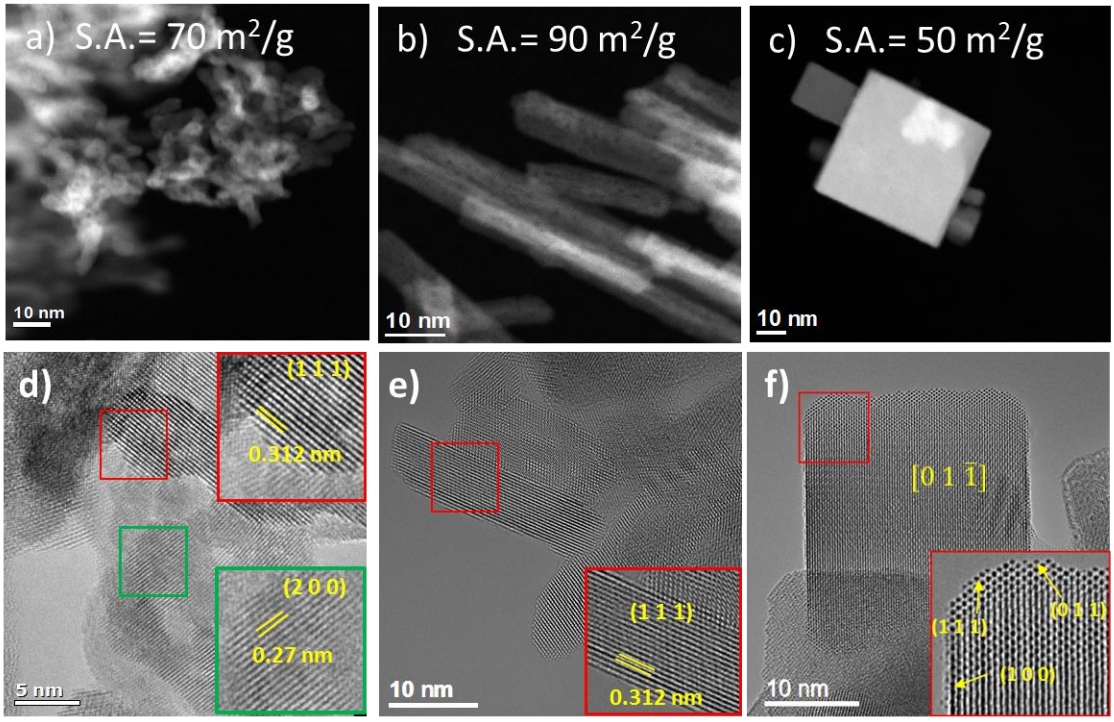

Figure 8. STEM and BET surface area on CeO2 a) polyhedra, b) rods, c) cubes, and HR-TEM on d) polyhedra, e) rods, f) cubes

SEM images were also taken of the CeO_2 rods and the cubes before and after aging in order to see the effect of aging on the morphology of these shapes. These samples were prepared on a double sided carbon tape mounted on an aluminum boat and are included in the supporting information (S1). Images were collected on a Hitachi 5200HR Scanning Electron Microscope (resolution of 2 nm).

The weight loading of the Pt/La-Al_2O_3 was determined by SEM fitted with EDS. Five scans were taken on the FRESH and AGED Pt/La-Al_2O_3 and can be found in the supporting information (S2). The AGED Pt/La-Al_2O_3 was found to have an average of 0.8 wt.% Pt present. A second method using XRD was used to corroborate this weight loading and will be discussed in the experimental design section. All XRD data was collected using a Rigaku Smart Lab diffractometer using Cu K_α radiation and a Rigaku D/teX position-sensitive detector with a Nickel K_β filter. Scans were performed from 20˚ to 90˚ with a scan rate of 6.2 degrees/minute.

CO oxidation was used on both the FRESH and AGED Pt/La-Al_2O_3 samples. These experiments were performed using a Varian CP-4900 Micro-GC utilizing a TCD detector. These two samples were used as reference catalyst for the remaining catalysts synthesized. The samples were packed into a stainless steel u-tube reactor which was mounted inside an insulated oven. The powder samples were packed between quartz wool with a thermocouple placed in the reactor at the sample. CO oxidation conditions used 1.5ml/min CO, 1ml/min O_2, and 75ml/min He (~2%CO) with a ramp rate of 2°C/min and sampling preformed every 3 minutes.

CHAPTER 4 – EXPERIMENTAL DESIGN

4.1 INTRODUCTION

The project began following in a similar manner as Carrillo et al. by trying to trap Pt using an oxide. CeO_2 was chosen as it has shown promising results in keeping Pt in a dispersed form. This research is broken into 2 parts that will address the defined objectives of the study. Part 1 was to prove that CeO_2 nanoshapes would serve as a good

trap for Pt during aging at DOC operating conditions. Part 2 will further investigate the interactions Pt has with the different surface facets of CeO_2.

4.1 PART 1: PT/LA-AL_2O_3 MIXED WITH CEO_2

To test the trapping abilities of CeO_2, a physical mixture of Pt/La-Al_2O_3 and CeO_2 was made. This first sample had a 1:1 weight ratio and was aged at 800 ˚C in air for 10 hours. A second sample was made with an AGED Pt/La-Al_2O_3 and CeO_2. This sample was needed to insure X-rays were not being absorbed by CeO_2 and in affect, blocking the signal from Pt in the system. Figure 9 shows the XRD pattern obtained for these samples.

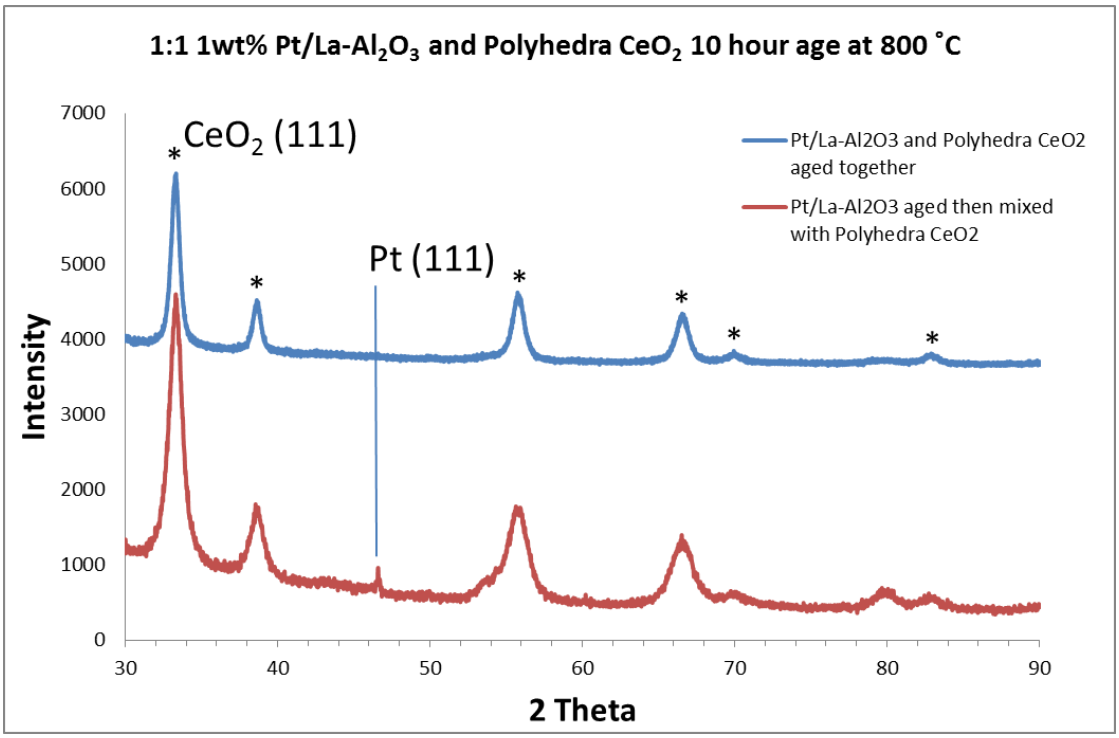

Figure 8: 1:1 weight ratio of Pt/Al2O3 and CeO2. Pattern collected with cobalt x-ray source leading to shift to the right.

The top pattern with the mixture of Pt/Al_2O_3 and CeO_2 aged together shows no peaks for Pt. While the bottom pattern where the Pt/La-Al_2O_3 has been aged, thus containing large

Pt particles, shows a peak for Pt. This led to the conclusion that CeO_2 was not blocking the whole Pt signal and the sample where Pt/Al_2O_3 and CeO_2 aged together must contain mostly dispersed Pt.

Two more weight ratios of Pt/Al_2O_3 and CeO_2 mixtures were tested to determine where a small Pt peak could be found in the samples aged together. A 10:1 and a 2:1 mixture of Pt/Al_2O_3 and CeO_2 where attempted and showed that Pt sintered dramatically in the 10:1 sample. The 2:1 sample however only showed a slight peak for Pt shown in supplemental information (S3). This led to the hypothesis that some Pt had formed larger particles while the rest had moved to the CeO_2 support and trapped in a dispersed phase.

After determining the weight ratio to be used in this study, 2:1 mixtures of Pt/Al_2O_3 and CeO_2 were prepared by grinding with a mortar and pestle FRESH 1 wt. % $Pt/La\text{-}Al_2O_3$ and each type of CeO_2. Each of the samples was loaded in a ceramic boat and placed in a quartz tube. The tube was put in a furnace and the samples aged at 800 ˚C for 10 hours in flowing air, denoted AGED Mix Cube, AGED Mix Rod, and AGED Mix Polyhedra. Figure 9 shows a schematic of this process. The three samples will be analyzed using XRD, TEM, SEM, and CO oxidation reaction. This would determine which surface facet of CeO_2 was more beneficial for trapping Pt in a dispersed phase.

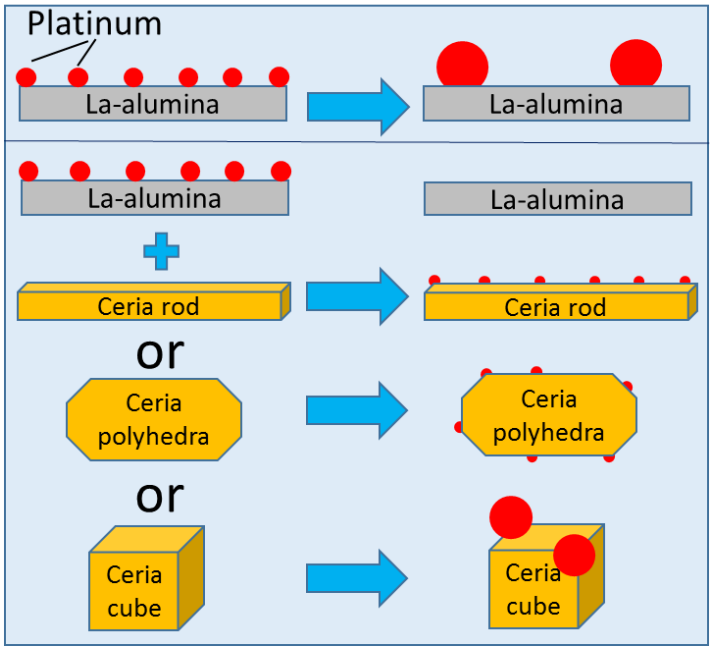

Figure 9: Schematic of Part 1 experiment to determine trapping ability of CeO_2 surface facets.

A fourth sample was also made in order to use XRD to find the weight loading of Pt in the samples. The fourth sample consisted of a 2:1 weight ratio of AGED 1 wt. % Pt on La-Al_2O_3 and polyhedra CeO_2. Using CeO_2 as an internal standard to measure the Pt peak against, a Rietveld refinement was performed and determined a loading of 0.8 wt.% Pt which matches the loading found by SEM-EDS. The XRD pattern for this process is included in the supporting information (S4)

4.2 PART 2: PT/CEO_2 NANOSHAPES

To further investigate the interactions between the different surface facets of CeO_2, modal catalysts were made containing only Pt and CeO_2. For each shape a 1 wt.% Pt on CeO_2 was synthesized using incipient wetness impregnation. These products were then left to dry in 80˚C air, followed by calcination in air at 350˚C for 5 hours. Each of the samples was then loaded in a ceramic boat and placed in a quartz tube. The tube was put in a furnace and the samples aged at 800 ˚C for 10 hours in flowing air. The

schematic in Figure 10 illustrates this process. Analysis using XRD, TEM, SEM, and CO oxidation was then carried out on the aged samples.

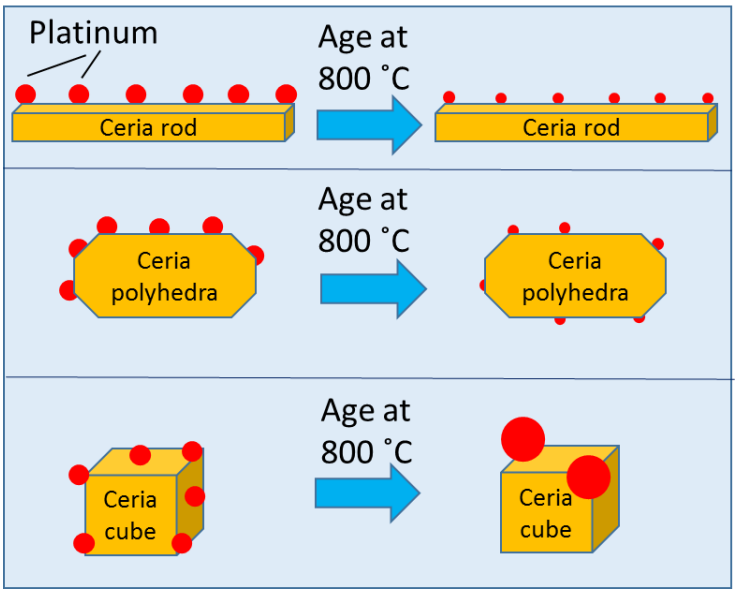

Figure 10: Schematic of Part 2 experiment to determine trapping ability of CeO_2 surface facets.

Other experiments were conducted on Pt weight loadings on CeO_2. These were used to determine if the lower surface area of the cubes could have affected the ability of Pt to be kept in a dispersed form rather than just having the (100) surface facet exposed.

CHAPTER 5 – RESULTS AND DISCUSSION

5.1 PART 1

5.1.1 XRD

Analysis of the XRD patterns from the three mixed sample catalysts shows different Pt (111) peaks for all samples. Figure 11 shows the three patterns obtained with an inset of the Pt (111) peak. All three patterns show a much smaller peak than the AGED 1 wt. % Pt on La-Al_2O_3 which would suggest that Pt has remained highly

dispersed or migrated to the CeO_2 in the samples and 'trapped.' The AGED Mix Cube sample has the largest peak indicative of having the most Pt in crystalline form. While the AGED Mix Rod sample has a smaller peak, the peak is more defined showing both $K_{\alpha 1}$ and $K_{\alpha 2}$. This would indicate less Pt is present in crystalline form than the AGED Mix Cube but there could be larger more defined particles present. The AGED Mix Polyhedra has the smallest and least defined peak of the three samples due to high dispersion of Pt and less present in a crystalline form. Using the Rietveld refinement method, the amount of crystalline Pt was found in each sample and reported in Table 1.

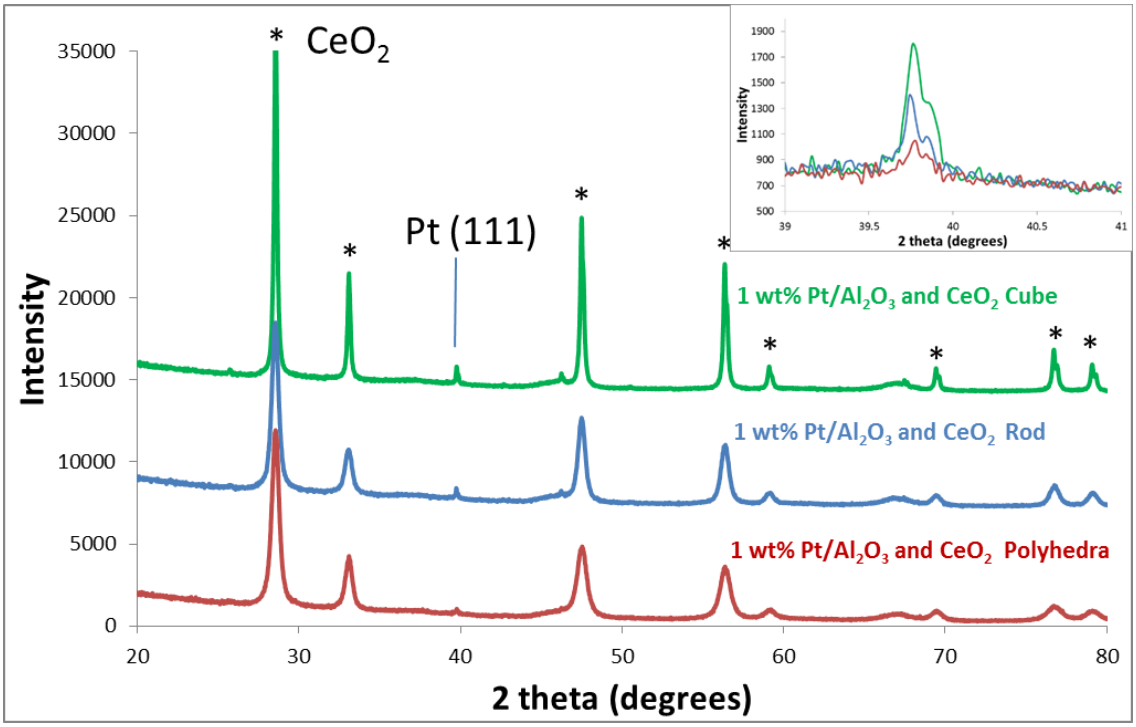

Figure 11. XRD patterns on AGED Mixed samples with inset of the Pt (1 1 1) peak.

Sample	wt.% Pt visible in XRD
Al_2O_3	0.81

Cube Ceria	0.60
Rod Ceria	0.34
Polyhedra Ceria	0.16

Table 1: wt.% Pt in crystalline form in 2:1 mixed samples

5.1.2 CO OXIDATION

Reaction data from CO oxidation experiments was used to verify the XRD data. Figure 12 shows the FRESH 1 wt. % Pt on La-Al_2O_3 and AGED 1 wt. % Pt on La-Al_2O_3 vs the three mixed samples prepared. The FRESH sample has good activity for the reaction due to the high dispersion of Pt particles. The AGED sample shows poor reactivity as all Pt is in crystalline form with few atoms on the surface of the Pt particles. The three mixed samples were all aged at 800 ˚C and show better reactivity than the AGED 1 wt. % Pt on La-Al_2O_3. We would have expected the AGED Mixed polyhedra to have better activity than the AGED Mixed rods due to more Pt present in a dispersed phase. These two samples actually light off at the same temperature with the polyhedra sample reaching 100% conversion of CO slightly faster. The AGED Mixed cubes do not perform as well as either of the samples as only 25% of the Pt in the sample is dispersed.

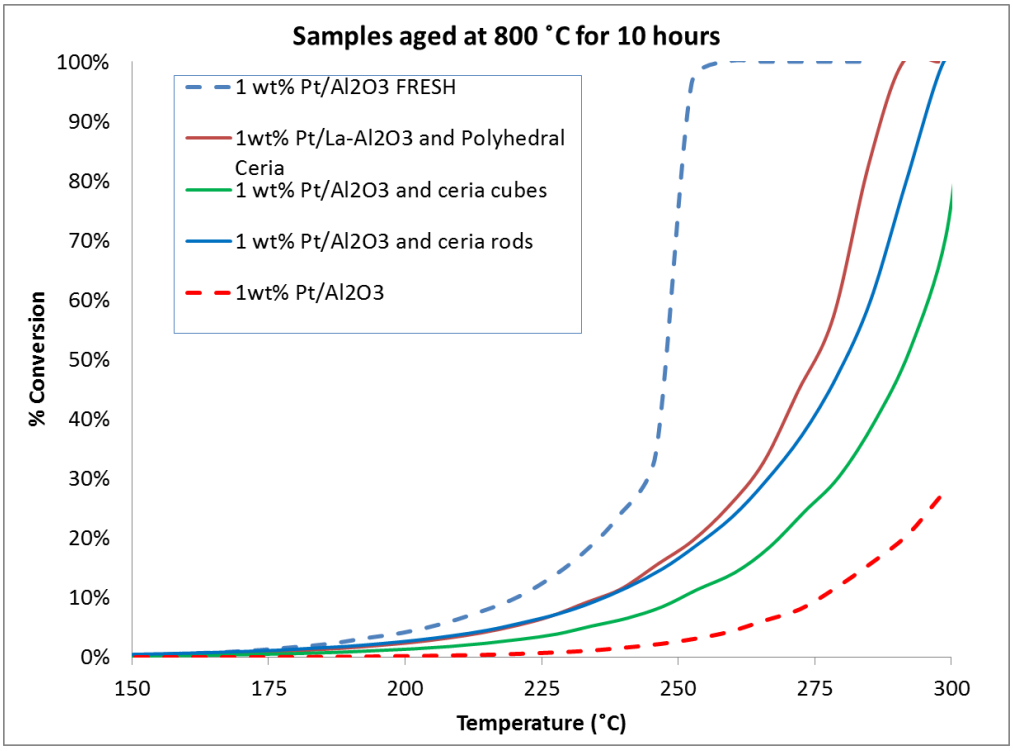

Figure 12. CO oxidation light off curves heating up to 300 C for Pt-Al_2O_3 and MIXED samples

Turn over frequency (TOF) was used for the Arrhenius plots. This allowed for a direct comparison of activation energies between samples. To do this, the flow of CO in the reaction had to be calculate and was found to be $8.55x10^{-7}$ mol/s. By using the values found from XRD for dispersed Pt in each sample, the number of moles of dispersed Pt could be calculated. This allowed the calculated activation energy to be normalized to the number of moles of Pt dispersed in each sample. Arrhenius plots for these samples along with activation energy and TOF can be found in supporting information S5, S6, S7. Nguyen et al. reported activation energy for CO oxidation of Pt-CeO_2 of 59 kJ/mol which correlates well with the collected results. [11] Data produced by Berlowitz et al. for a Pt (100) crystal with a diameter of 0.92 cm had similar activation energy at these temperatures. [12] The high dispersion of Pt on our catalysts was able to achieve the same activation energy with much less Pt.

5.1.3 TEM

The complex nature of this mixed system made it difficult for imaging. The contrast between Pt and Ce is minimal due to the close atomic weights. The capabilities of the JEOL 2010F 200kV made it difficult to locate Pt particles because of the similar contrasts and high level of dispersion of Pt. Figure 13 shows the AGED Mixed polyhedra. The support present is CeO_2 polyhedra with nm sized Pt dispersed on the surface.

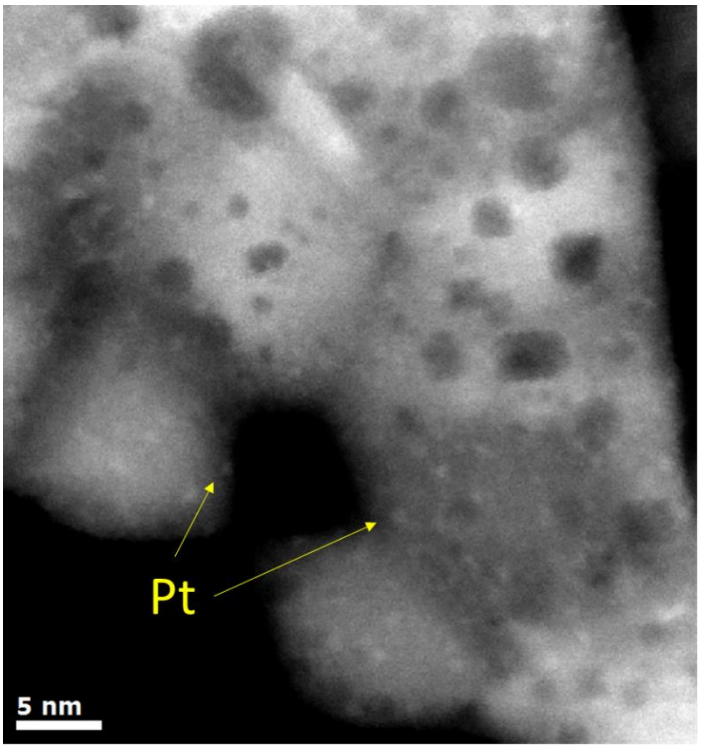

Figure 13: TEM of AGED Mixed polyhedra with highly dispersed Pt after aging at 800 ˚C for 10 hours

5.1.4 ADDITIONAL AGING

Further aging was carried out on the mixed polyhedra sample. The expected result of further aging would be a loss of Pt as a vapor or by sintering. Interestingly this was not the case. After aging the sample at 800 ˚C for one week, the Pt(111) peak in XRD

became smaller and the CO oxidation reactivity was lighting off at a lower temperature as shown in supporting information (S8, S9). This would indicate that some redispersion of Pt is occurring in the sample instead of sintering.

5.2 PART 2

5.2.1 XRD

To further our knowledge of the trapping characteristics of the different surface facets of CeO_2, the three AGED 1 wt.% Pt/CeO_2 samples were tested as well. XRD was utilized again as a preliminary test to see if there had been Pt particle growth after aging. Figure 14 shows the three XRD spectra collected along with SEM images of the samples. In the 1 wt.% Pt on CeO_2 cube, a small peak can be seen at ~ 40° corresponding to Pt (111). This Pt peak indicates that the dispersed Pt has sintered and formed larger particles. No peak for Pt is present in either the polyhedra or rod samples. The corresponding SEM pictures show large particle of Pt (~300 nm) present in the cube sample. Pt particles could not be seen in the polyhedra or rod sample due to the high dispersion of Pt.

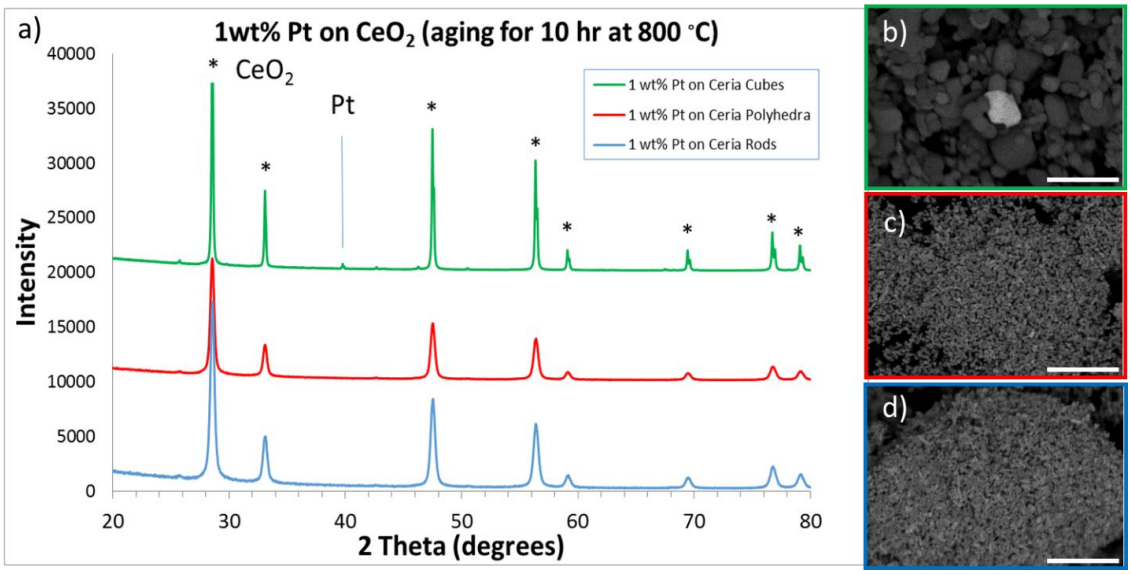

Figure 14. a) XRD on 1 wt.% Pt on CeO_2 after aging for 10hr at 800 C. SEM images are shown for b) 1 wt.% Pt on CeO_2 cubes, c) 1 wt.% Pt on CeO_2 polyhedra, d) 1 wt.% Pt on CeO_2 rods. Scale bars are 500 nm

5.2.2 CO OXIDATION

CO oxidation experiments were also carried out on the 1 wt.% Pt/CeO_2 samples. Figure 15 shows the light off curves for these experiments. Interestingly the CeO_2 rods were lighting off before the CeO_2 polyhedra, unlike the AGED Mixed samples. As both samples have the same amount of dispersed Pt in them, we believe the rods predominant facet being the (111) is promoting this. The CeO_2 cubes still remained the least active of the Pt/CeO_2 samples but still more active than the AGED Pt/Al_2O_3 sample.

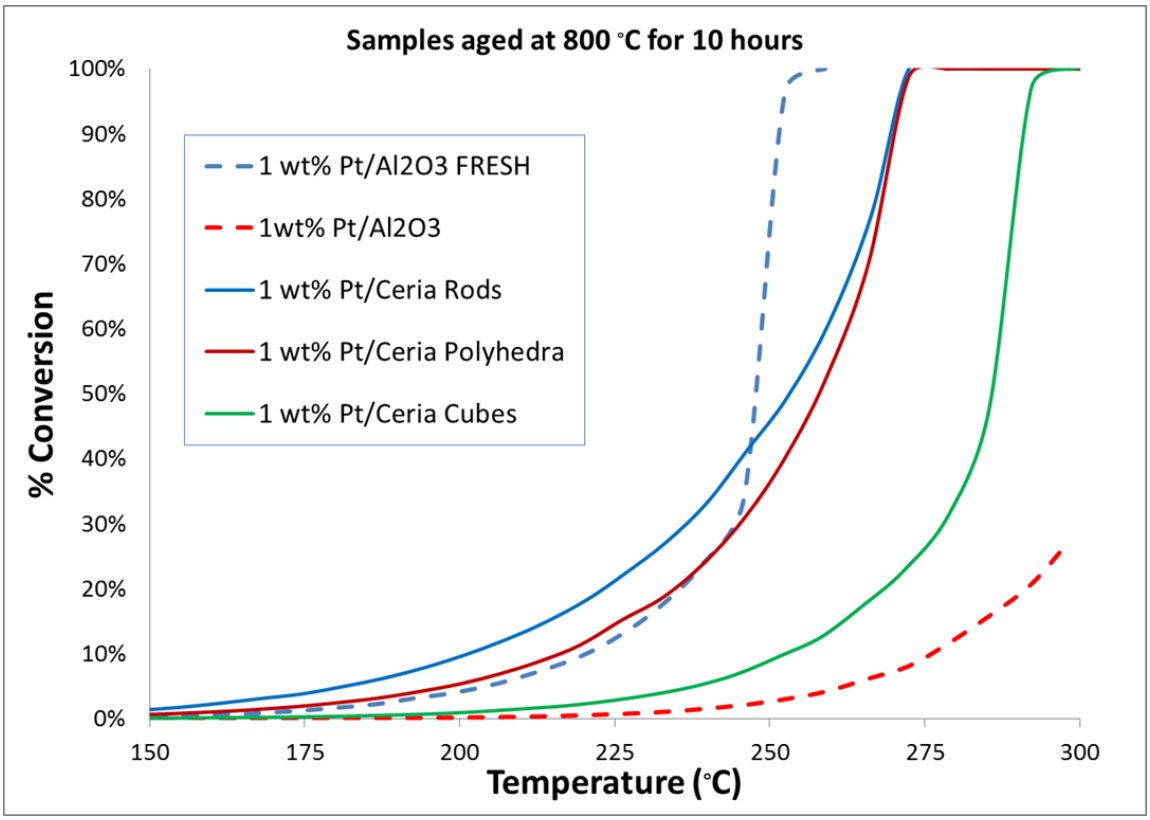

Figure 15. CO oxidation light off curves heating up to 300 C for Pt-Al_2O_3 and MIXED samples

5.2.3 TEM

TEM images were taken of the AGED 1 wt.% Pt on CeO_2 rods and polyhedra to confirm that Pt was present in a highly dispersed form. The images in Figure 16 were captured using a JEOL JEM ARMS200CF 200 kV aberration-corrected (AC) transmission electron microscope (resolution of 0.08 nm). Pt particles are visible in both samples to be less than 1 nm. This indicates the Pt is atomically dispersed which is why no Pt peak was present in the XRD spectra. The Pt particles slightly larger than 1 nm we believe formed while the electron beam from the TEM was placed on the sample.

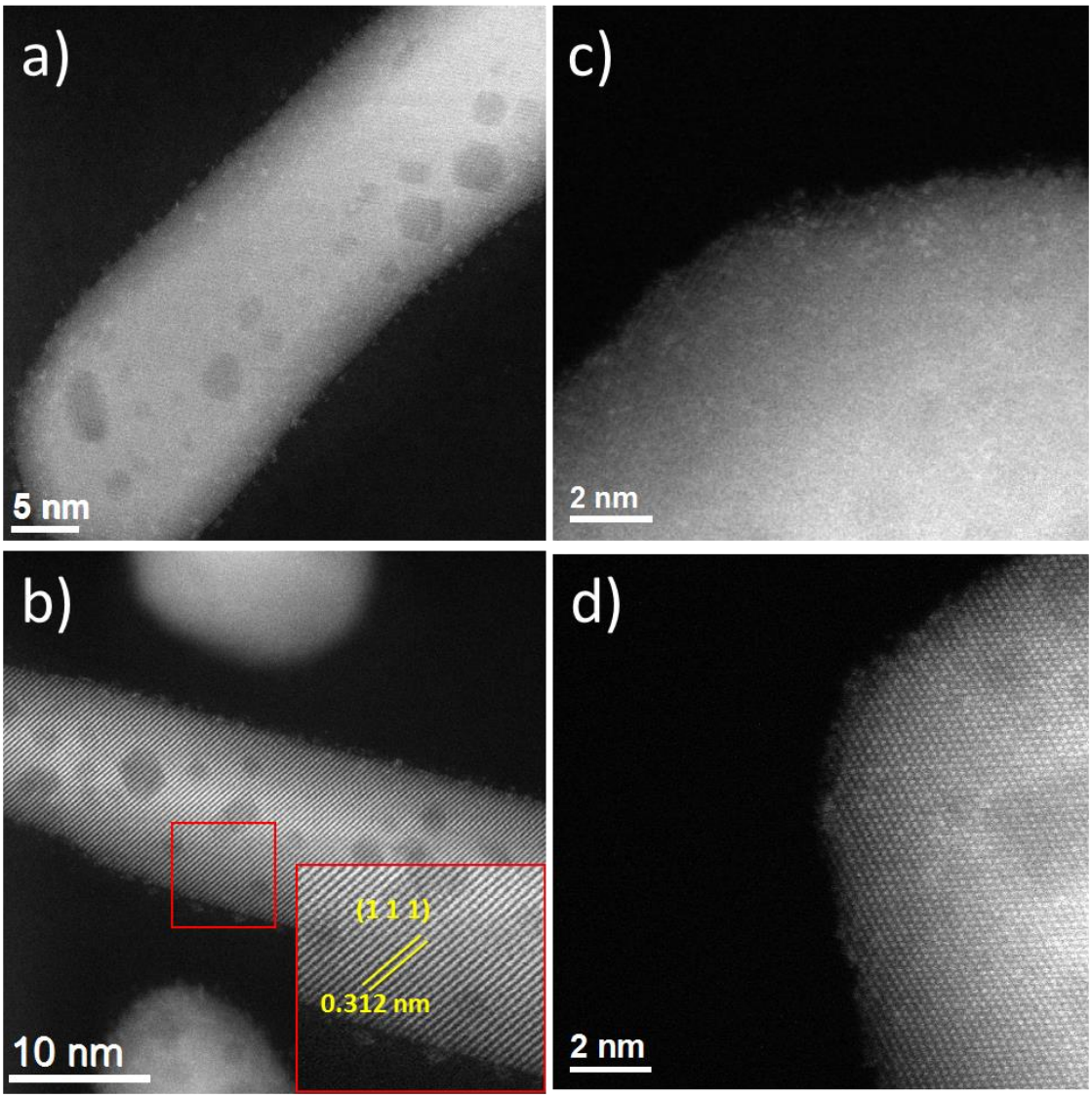

Figure 16. AC-TEM on 1 wt.% Pt-CeO_2 RODS a and b AND POLYHEDRA c and d

TEM images were also taken of the AGED Pt/CeO_2 cube sample. Figure 17 shows no Pt particles are present on the cubes. Combining this information with the SEM image from Figure 14 that shows a Pt particle of ~300 nm, and the lower CO oxidation reactivity, we have concluded that most of the Pt in the sample has sintered and formed larger particles.

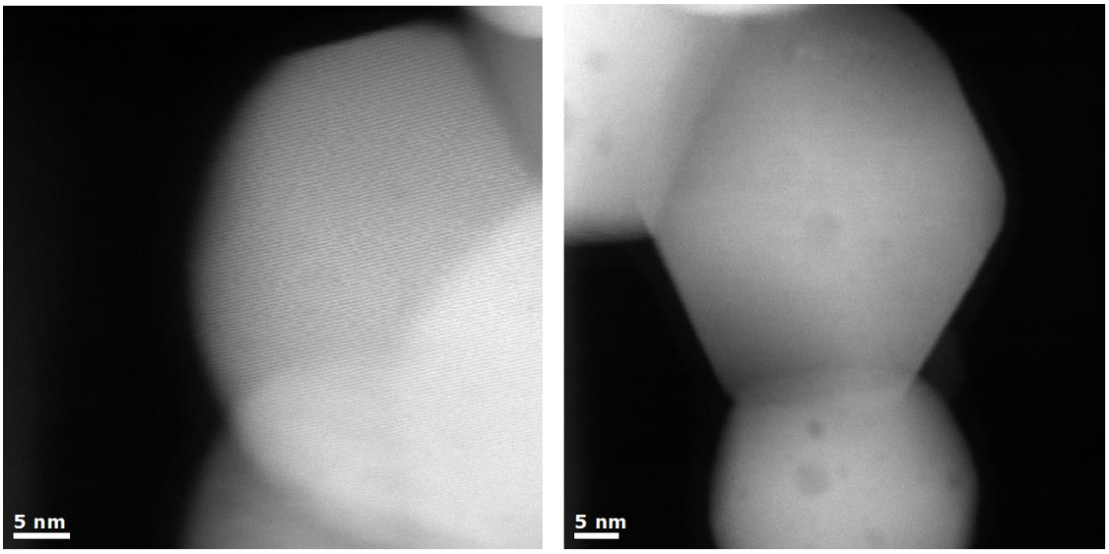

Figure 17: TEM on Pt/CeO_2 cubes

5.2.4 PT WEIGHT LOADING ON CEO_2

A concern brought up during Part 2 was if the lower surface area of the cubes was affecting the ability to trap Pt. If all the sites where Pt could be trapped are occupied, would Pt begin to nucleate at certain sites and pull other Pt atoms to them during aging? To test this idea different weight loadings (1-6%) of Pt were on CeO2 polyhedra were made. These samples were then aged at 800 ˚C in air for 10 hours. These samples were then characterized using XRD, TEM, SEM and BET.

The XRD data showed no Pt peak after aging until 5 wt.% shown in Figure 18. This would indicate that CeO_2 was able to keep Pt dispersed until just before 5 wt.%. Pt also was stabilizing CeO_2 from sintering as shown in the BET surface areas reported in supporting information S10. At 6 wt.% a large peak in XRD was present and BET surface area dropped dramatically.

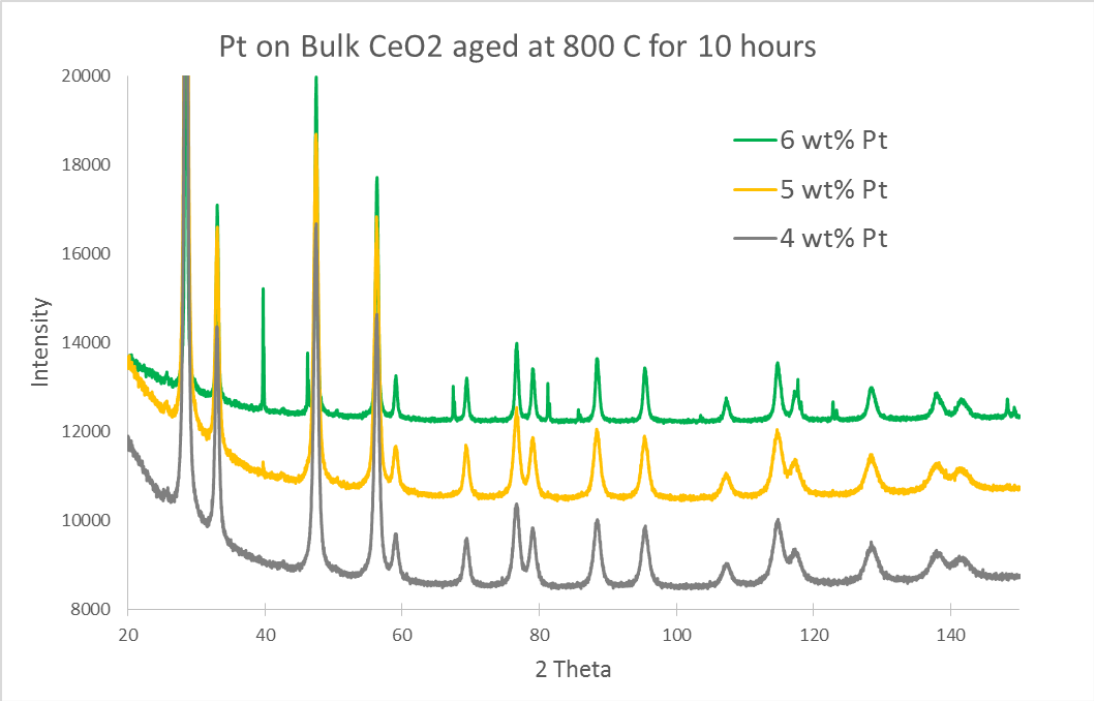

Figure 18: XRD on various weight loadings of Pt/CeO_2 aged at 800 ˚C for 10 hours.

TEM and SEM images of the 6 wt.% Pt/CeO_2 sample were taken to see if a bimodal distribution of large Pt particles and a dispersed form were present in the sample. As shown in Figure 19, both large particles and a dispersed phase are present in the sample. In Figure 19 a) and b) Pt particles of 3 to 5 nm are easily visible by TEM. Figure 19 c) with a zoomed in image in d) show Pt particles up to 2 microns in size. This is quite different than the Pt/CeO_2 cube sample where no dispersed phase was present.

CHAPTER 6 – SUMMARY AND CONCLUSIONS

6.1 SUMMARY

Three types of CeO_2 exposing different surface facets were used in this study of trapping Pt. These supports were characterized by TEM and HR-TEM and indexed to insure they were displaying the desired facets.

In Part 1, a 2:1 mixture was then made with Pt/La-Al_2O_3 and each CeO_2 support, followed by aging at 800 ˚C for 10 hours. After aging, the samples were characterized using XRD, TEM, SEM and CO oxidation to see if CeO_2 was able to trap Pt in a dispersed phase.

In Part 2, Pt was deposited directly onto each of the CeO_2 supports. These samples were then aged at 800 ˚C for 10 hours and characterized using XRD, TEM, SEM, and CO oxidation. This allowed for further investigation into the interactions between Pt and the different surface facets of each support.

6.2 CONCLUSIONS

CeO_2 has been shown in the past to be able to bind Pt and reduce the effect of sintering during aging at high temperature. [5, 13, 14] The study performed here has clearly indicated that the different surface facets of CeO_2 nanoshapes can provide varying levels of sintering inhibition. The (100) facet present on CeO_2 cubes has proved ineffective at trapping Pt in a dispersed form.

Although, the cubes do perform better than AGED Pt/La-Al_2O_3, they are much less active in CO oxidation experiments, and even allow the growth of large Pt particles of up to 2 μm. The (111) facet present on CeO_2 rods and polyhedra exhibit great trapping characteristics for Pt. This observation has been well characterized with an XRD study showing very small peaks for Pt after aging in mixed samples with CeO_2 rods and polyhedra. These results are corroborated by the Pt/CeO_2 samples containing rods and polyhedra where no Pt peak is present after aging at 800 ˚C.

CO oxidation experiments have also shown the benefit CeO_2 rods and polyhedra have on keeping Pt the most active. This is done by trapping Pt in a highly dispersed form. Lastly TEM images on Pt/CeO_2 rods and polyhedra show a highly dispersed Pt after aging and no large Pt particles. SEM images on the same samples show no large particles while Pt particles of up to 2 μm can be located easily in the CeO_2 cube sample.

Supporting Information

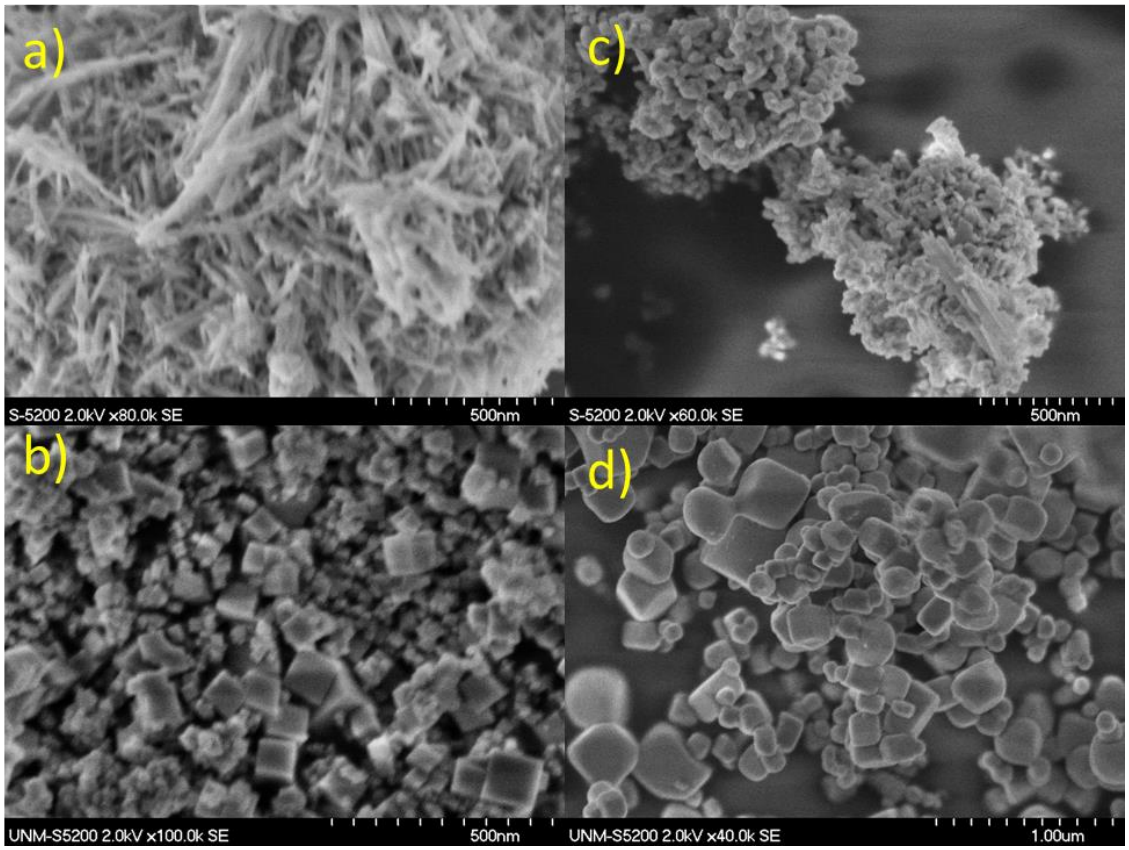

Supporting 1. SEM images on Fresh a) CeO_2 rods, b) CeO_2 cubes, and Aged at 800 C for 10 hours c) CeO_2 rods, d) CeO_2 cubes

Spectrum	Pt wt.% on FRESH La-Al_2O_3	Pt wt.% on La-Al_2O_3 Aged 800 ˚C
1	1.2	0.9
2	1.2	0.8
3	1.3	0.8
4	1.0	1.0
5	1.0	0.5
Average	1.14	0.8

Supporting 2. Pt wt.% on La-Al2O3 collected from SEM with EDS system on both FRESH and AGED samples

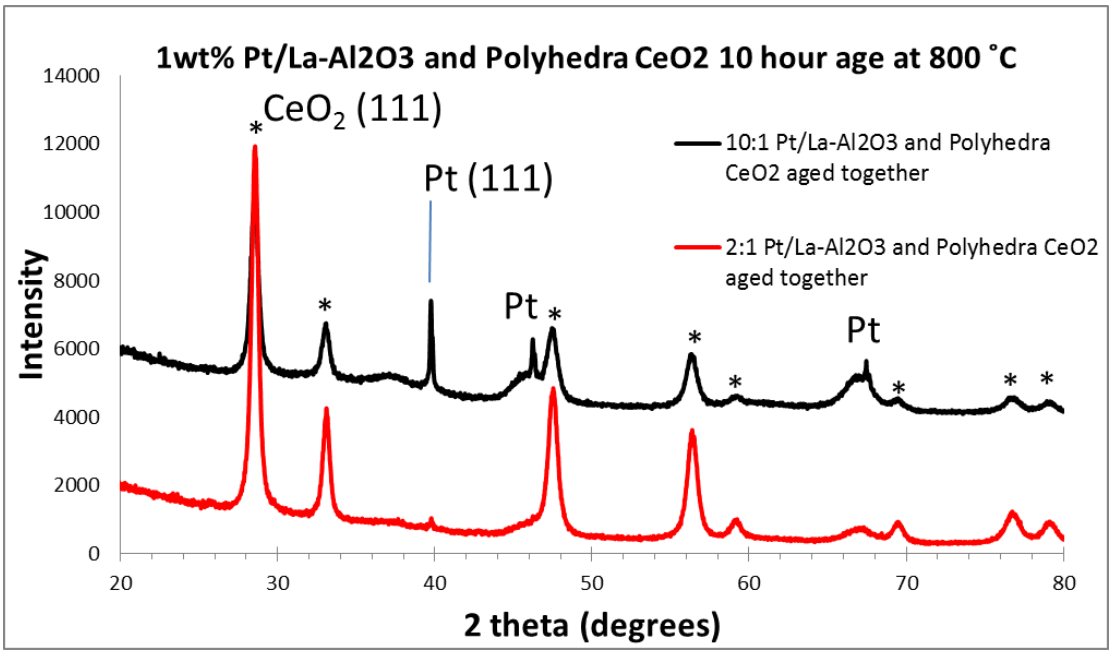

Supporting 3. XRD on 10:1 and 2:1 weight ratios of Pt/Al_2O_3 and CeO_2 aged together

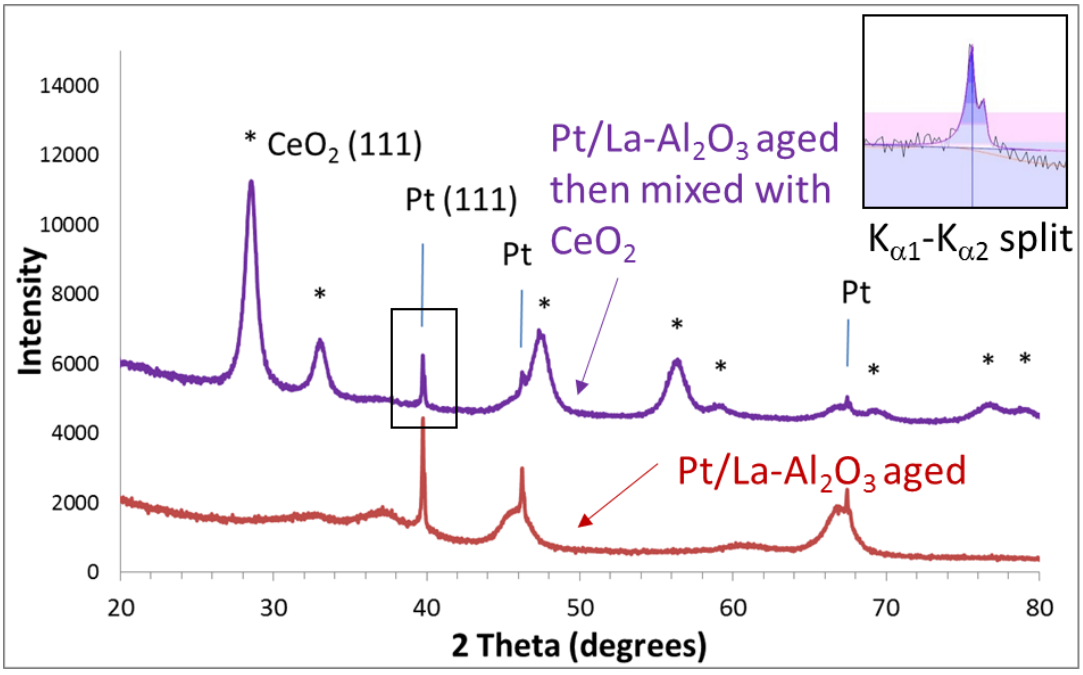

Supporting 4. Samples used to quantify fraction of Pt visible to XRD (Pt in crystalline form)

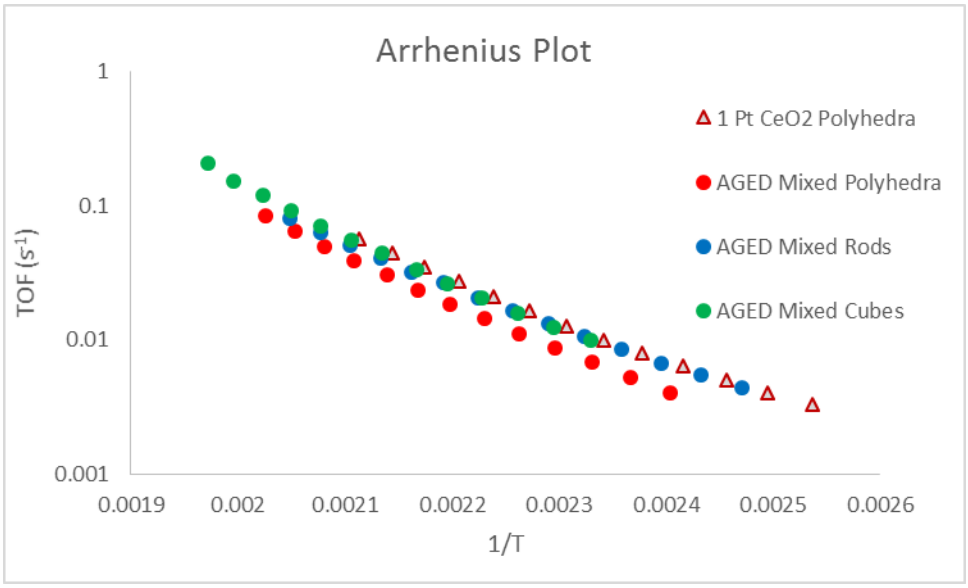

Supporting 5. Arrhenius Plot used to calculate activation energy

Sample	E_a (kJ/mol)
Pt-CeO2 Polyhedra	56.44
2 to 1 Mixed Polyhedra	66.58
2 to 1 Mixed Rod	57.18
2 to 1 Mixed Cube	70.06
Nguyen Pt-CeO2 [11]	59
Berlowitz Pt (1 0 0) Crystal Temperature <170 °C [12]	54.3
Berlowitz Pt (1 0 0) Crystal Temperature >230 °C [12]	137.7

Supporting 6. Activation Energies

Sample	TOF (s^{-1}) at 200 ˚C	Conversion at 200 ˚C	TOF (s^{-1}) at 225 ˚C	Conversion at 225 ˚C
2 to 1 Mixed Polyhedra	$3.89x10^{-2}$	2.46%	$1.09x10^{-1}$	6.86%
2 to 1 Mixed Rod	$5.07x10^{-2}$	2.86%	$1.29x10^{-1}$	7.29%
2 to 1 Mixed Cube	$5.59x10^{-2}$	1.41%	$1.54x10^{-1}$	3.88%

Supporting 7. CO oxidation TOF and conversion data

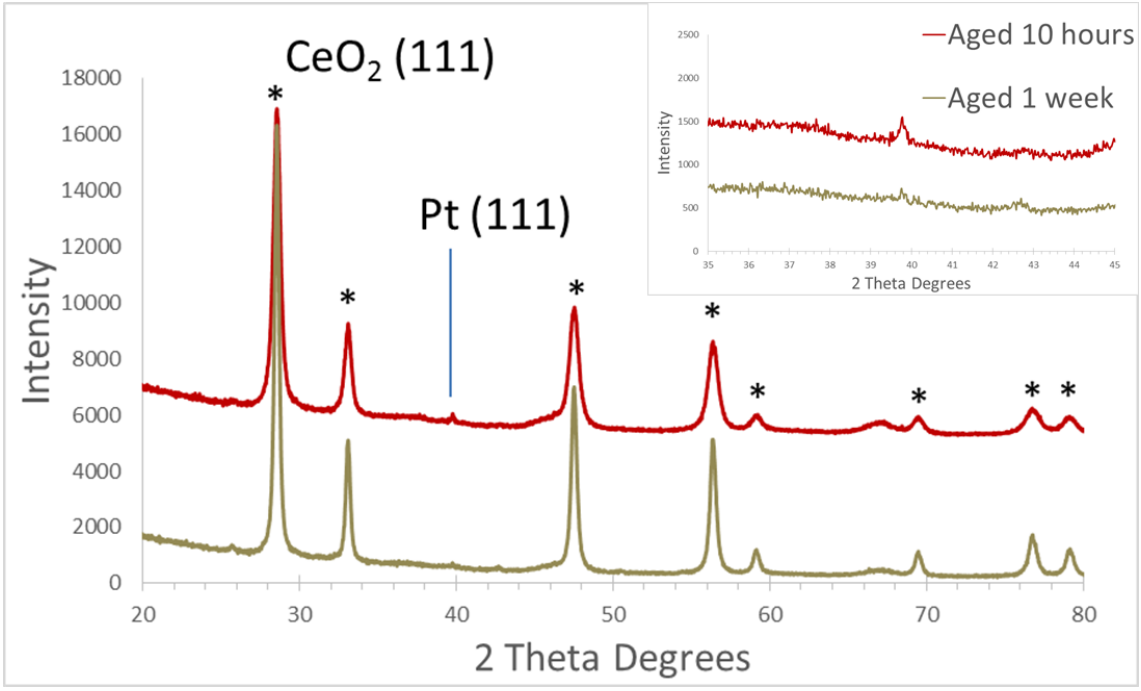

Supporting 8. XRD of 2:1 Mixed polyhedra samples aging for 10 hours and 1 week at 800 ˚C, inset of Pt (111)

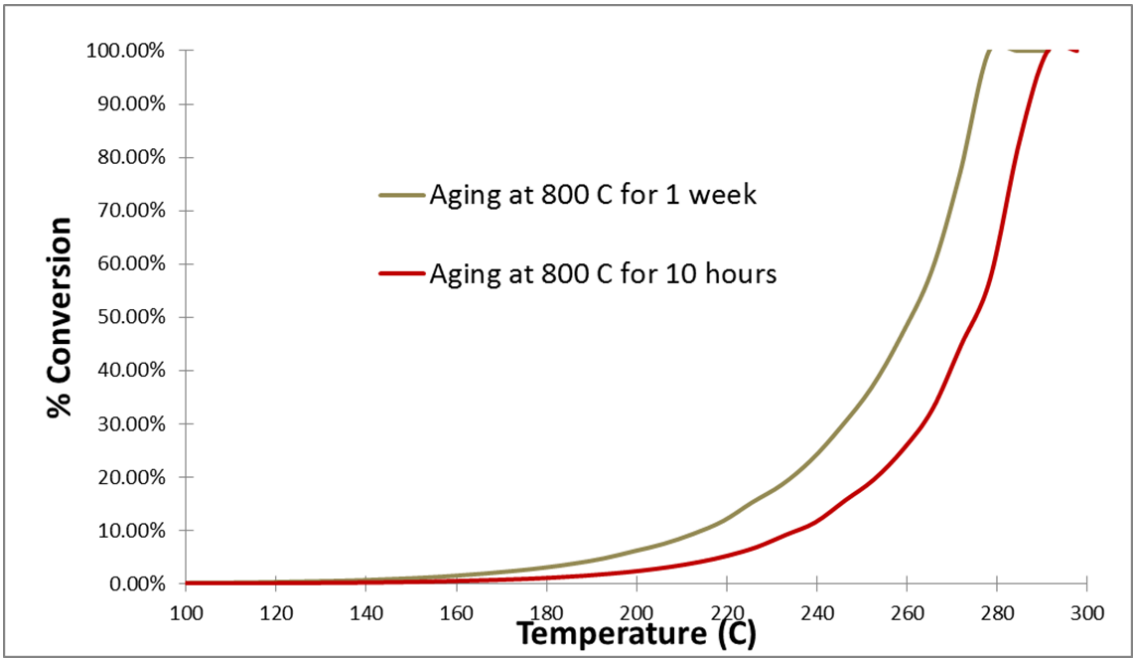

Supporting 9. CO oxidation of 2:1 Mixed polyhedra samples aging for 10 hours and 1 week at 800 ˚C

Pt loadings	**BET S.A. (m^2/g)**
1 wt% Pt (fresh)	110.60
1 wt% Pt (aged)	29.46
4 wt% Pt (fresh)	81.31
4 wt% Pt (aged)	51.00
5 wt% Pt (fresh)	82.05
5 wt% Pt (aged)	46.18
6 wt% Pt (fresh)	89.22
6 wt% Pt (aged)	25.67

Supporting 10. BET surface areas for FRESH and AGED Pt/CeO_2

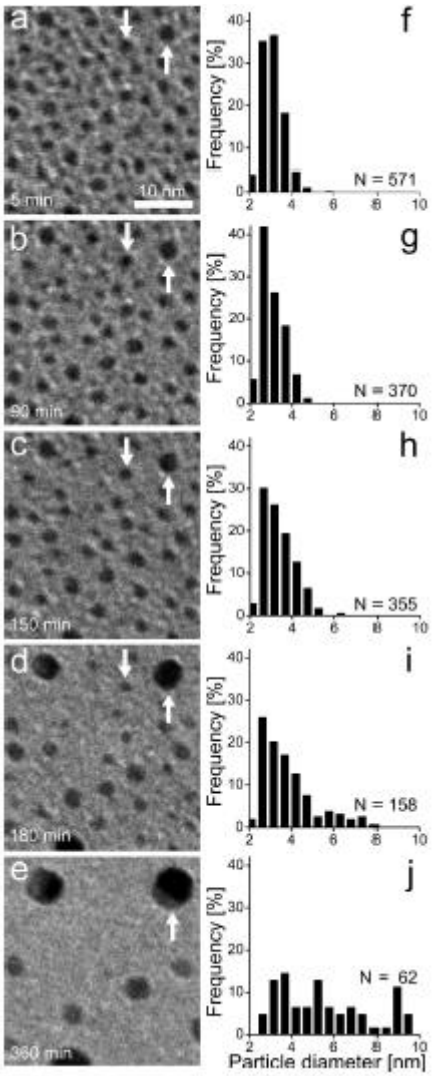

Supporting 11. Oswald Ripening of Pt nanoparticles on Al_2O_3 support with particle distributions.[22]

REFERENCES

1. Hansen, T.; Datye, A. Sintering of Catalytic Nanoparticles: Particle Migration or Ostwald Ripening. *Accounts of Chemical Research*. **2012**. 46. 1720-1730.

2. Graham, G.; McCabe, R. Coarsening of Pt particles in a model NO_x trap. *Catalysis Letters*. **2004**. 93.

3. Johns, T.; Datye, A. Microstructure of Bimetallic Pt-Pd Catalysts under Oxidizing Conditions. *ChemCatChem*. **2013**. 5. 2636-2645.

4. Carrillo, C.; Datye, A. Trapping of Mobile Pt Species by PdO Nanoparticles under Oxidizing Conditions. *J. Phys. Chem. Lett*. **2014**. 5. 2089-2093.

5. Nagai, Y.; Matsumoto, S. Sintering inhibition mechanism of platinum supported on ceria-based oxide and Pt-oxide–support interaction. *Journal of Catalysis*. **2006**. 242. 103-109.

6. Wu, T.; Yang, X. Investigation of the Redispersion of Pt Nanoparticles on Polyhedral Ceria Nanoparticles. *J. Phys. Chem. Lett*. **2014**. 5. 2479-2483.

7. Bruix, A.; Neyman, K. Maximum Noble-Metal Efficiency in Catalytic Materials: Atomically Dispersed Surface Platinum. *Angew. Chem. Int. Ed.* **2014**. 53. 10525-10530

8. Yamamoto, T.; Funabiki, T. Structures and Acid-Base Properties of La/Al_2O_3 – Role of La Addition to Enhance Thermal Stability of γ-Al_2O_3. *Chem. Mater*. **2003**. 15. 4830-4840.

9. Gaudet, J.; Datye, A. Improved Low-Temperature CO Oxidation Performance of Pd Supported on La-Stabilized Alumina. *ACS Catalysis*. **2013**. 3. 846-855.

10. Mai, H.; Yan, C. Shape-Selective Synthesis and Oxygen Storage Behavior of Ceria Nanopolyhedra, Nanorods, and Nanocubes. *J. Phys. Chem. B.* **2005**. 109. 24380-24385.

11. Nguyen, T.; Piccolo, L. Trends in the CO oxidation and PROX performances of the platinum-group metals supported on ceria. *Catalysis Today*. **2015**. 253. 106-114.

12. Berlowitz, P.; Goodman, W. Kinetics of CO Oxidation on Single-Crystal Pd, Pt, and Ir. *J. Phys. Chem*. **1988**. 92. 5213-5221.

13. Nagai, Y.; Matsumoto, S. In Situ Redispersion of Platinum Autoexhaust Catalysts: An On-Line Approach to Increasing Catalyst Lifetimes. *Angew. Chem. Int. Ed*. **2008**. 47. 9303–9306.

14. Luo, J.; Li, Wei. Low Temperature Ceria-Based Lean NO_x Traps. Catalysis Letter. **2012**.
15. Bera, P.; Subbanna, G. Ionic Dispersion of Pt over CeO2 by the Combustion Method: Structural Investigation by XRD, TEM, XPS, and EXAFS. *Chem. Mater*. **2003**. 15. 2049-2060.

16. Souza, R.; Horner, S. Modifying the barriers for oxygen-vacancy migration in fluorite-structured CeO2 electrolytes through strain: a computer simulation study. *Energy Environ. Sci*. **2012**. 5. 5445

17. Nolan, M., Watson, G. Density functional theory studies of the structure and electronic structure of pure and defective low index surfaces of ceria. *Surface Science.* **2005**. 576. 217–229.

18. Lin, Y., Marks, L. Imaging the Atomic Surface Structures of CeO_2 Nanoparticles. *Nano Letters*. **2013**. 14. 191-196.

19. Wang, Z., Feng, X. Polyhedral Shapes of CeO2 Nanoparticles. *J. Phys. Chem. B.* **2003**. 107. 13563-13566.

20. Kinch, R., Ishikawa, Y. A Density-Functional Theory Study of the Water-Gas Shift Mechanism on Pt/Ceria(111). *J. Phys. Chem. C*. **2009**. 113. 9239–9250.

21. Esch, F., Rosei, R. Electron Localization Determines Defect Formation on Ceria Substrates. *Science*. **2005**. 309. 752-755.

22. Simonsen, S., Helveg, S. Direct Observations of Oxygen-induced Platinum Nanoparticles Ripening Studied by In Situ TEM. *JACS*. **2010**. 132. 7968-7975.

23. Brunelle, J. Preparation of Catalysts by Metallic Complex Adsorption on Mineral Oxides. *Pure and Appl. Chem.* **1978**. 50. 1211-1229.

24. Fogler, H. Elements of Chemical Reaction Engineering. Fourth Edition. Prentice Hall. 2006.